CCP_24

by Pranowo Pranowo

Submission date: 01-Aug-2019 01:26PM (UTC+0700)
Submission ID: 1156710717
File name: Steady_and_Unsteady_Incompressible_Navier_Stokes_Equations.doc (1.59M)
Word count: 2418
Character count: 13213

Discontinuous Galerkin Method for Solving Steady and Unsteady Incompressible Navier Stokes Equations

Pranowo[a,b], A. Gatot Bintoro[c], & Deendarlianto[d]

[a]Ph.D. Student of the Department of Electrical Engineering, Faculty of Engineering, Gadjah Mada University, Jalan Grafika No. 2, Yogyakarta 55281, Indonesia

[b]Lecturer of the Department of Informatics Engineering, Yogyakarta Atma Jaya University, Jl. Babarsari 43, Yogyakarta 55281, Indonesia.
Email: pran@mail.uajy.ac.id

[c]Lecturer of the Department of Industrial Engineering, Yogyakarta Atma Jaya University, Jl. Babarsari 43, Yogyakarta 55281, Indonesia.

[d]Lecturer of the Department of Mechanical and Industrial Engineering, Gadjah Mada University, Jalan Grafika No. 2, Yogyakarta 55281, Indonesia

ABSTRACT

Purpose: *To develop high order discontinuous galerkin method for solving steady and unsteady incompressible flow based on artificial compressibility method.*
Design/methodology/approach: *This paper uses discontinuous galerkin finite element procedure which is based on the artificial compressibility technique in connection with a dual time stepping approach. A second order implicit discretization is applied to achieve the required accuracy in real time while an explicit low storage fourth order Runge Kutta scheme is used to march in the pseudo-time domain. A nodal high order discontinuous galerkin finite element is used for the spatial discretization.*
Findings: *Provides stable and accurate methods for solving incompressible viscous flows compared with previous numerical results and experimental results.*
Research limitations: *It is limited to two-dimensional steady and unsteady laminar viscous flow.*
Practical implications *– A very useful source of information and favorable advice for people is applied to piping system and low speed aerodynamics.*
Originality: *This works presents an extension of the previous work of [1] and [2] to time and space accurate method for solving unsteady incompressible flows.*

Keywords: *steady and unsteady flows, discontinuous galerkin, artificial compressibility.*

1. INTRODUCTION

Numerical Solutions of the incompressible Navier-Stokes equations are of interest in many engineering applications. Problems which can be addressed by incompressible Navier-Stokes equations include internal flows, hydrodynamics flows, low speed aerodynamics and external flows. There is a continuing interest in finding solution methodologies which will produce accurate results in time and space. The problem of coupling changes in the velocity field with changes in pressure field while satisfying the continuity equation is the main difficulty in obtaining solutions to the incompressible Navier-Stokes.

There are two types of method using primitive variables which have been developed to solve the equations. The first type of methods can be classified as pressure-based methods. In these methods, the pressure field is solved by combining the momentum and mass continuity equations for form a pressure or pressure-correction equation. The second type of methods employs the artificial compressibility (AC) formulation. This idea was first introduced by Chorin [3] and extensively used by other researchers since. In this method, a pseudo-temporal pressure terms is added to continuity equation to impose the incompressibility constraint. Several authors have employed this method successfully in computing unsteady problems.

The original version of the AC method is only accurate for steady-state solutions to the incompressible flows [4, 5], however there are some efforts which conducted to solve unsteady flows using dual time stepping AC method. Reference [6] used third order flux difference technique for convective terms and second-order central difference for viscous terms. The semi discrete equations are solved implicitly by using block line-relaxation scheme. Reference [1] used finite element method for spatial discretization. A second-order discretization is employed in real time while an explicit multistage Runge Kutta is used to march in pseudo time domain.

This work presents an extension of the previous work of [1, 2] to time and space accurate method for solving unsteady incompressible flows. A nodal high order discontinuous galerkin finite element is used for the spatial discretization a second order implicit discretization is applied to achieve the required accuracy in real time while an explicit low storage fourth order Runge Kutta scheme is used to march in the pseudo-time domain. The computed results show accuracy of the code by presenting the steady and unsteady flow past a 2-dimensional circular cylinder.

2. PROBLEM DESCRIPTION

Artificial compressibility method is introduced by adding a time derivative of pressure to the continuity equation. In the steady-state formulation, the equations are marched in a time-like fashion until the divergence of velocity vanishes. The time variable for this process no longer represents physical time. Therefore, in the momentum equations t is replaced with τ , which can be thought of as an artificial time or iteration parameter [7]. As a result, the governing equations can be written in the following form:

$$\frac{\partial \mathbf{U}}{\partial \tau}+\frac{\partial \mathbf{F}^j}{\partial x_j}+\frac{\partial \mathbf{G}^j}{\partial x_j}=0\,, \quad j=1,2 \tag{1}$$

Where

$$\mathbf{U}=\begin{bmatrix} p \\ u_1 \\ u_2 \end{bmatrix} \quad \mathbf{F}^j=\begin{bmatrix} \varepsilon^2 u_j \\ u_i u_j+p\delta_{1j} \\ u_2 u_j+p\delta_{2j} \end{bmatrix} \tag{2}$$

$$\mathbf{G}^j=\begin{bmatrix} 0 \\ \tau_{1j} \\ \tau_{2j} \end{bmatrix} \qquad \tau_{ij}=\frac{1}{\mathrm{Re}}\left(\frac{\partial u_i}{\partial x_j}+\frac{\partial u_j}{\partial x_i}\right)$$

In these equations, τ is the artificial time variable, u_i is the velocity in direction x_i, p is the pressure, τ_{ij} is stress tensor, ε is an artificial compressibility parameter, δ_{ij} is Kronecker delta and Re is the Reynolds number.

The extension of artificial compressibility method to unsteady flow is introduced by adding physical time derivative of velocity components to 2 momentum equations in Equations (2) [6, 1]. The obtained equations can be written as:

$$\frac{\partial \mathbf{U}}{\partial \tau}+\mathbf{I}^M\frac{\partial \mathbf{U}}{\partial t}+\frac{\partial \mathbf{F}^j}{\partial x_j}+\frac{\partial \mathbf{G}^j}{\partial x_j}=0\,, \quad j=1,2 \tag{3}$$

Where $\mathbf{I}^M=\begin{bmatrix} 0 & 0 & 0 \\ 0 & 1 & 0 \\ 0 & 0 & 1 \end{bmatrix}$

3. DISCRETIZATION

The spatial derivatives are discretized by using a discontinuous galerkin method. The simplified of Eq. (3) according to Galerkin's procedure using the same basis function ϕ within each element is defined below:

$$\begin{aligned} &\left(\phi,\frac{\partial \mathbf{U}}{\partial \tau}+\mathbf{I}^M\frac{\partial \mathbf{U}}{\partial t}+\frac{\partial \mathbf{F}^j}{\partial x_j}+\frac{\partial \mathbf{G}^j}{\partial x_j}\right)=0 \\ &\Leftrightarrow\left(\phi,\frac{\partial \mathbf{U}}{\partial \tau}+\mathbf{I}^M\frac{\partial \mathbf{U}}{\partial t}\right)_\Omega+\left(\phi,n_j\mathbf{F}^j+n_j\mathbf{G}^j\right)_{\partial\Omega} \\ &-\left(\frac{\partial}{\partial x}\phi,\mathbf{F}^j\right)_\Omega-\left(\frac{\partial}{\partial x}\phi,\mathbf{G}^j\right)_\Omega=0 \end{aligned} \tag{4}$$

Integrate by parts again equation (4):

$$\begin{aligned} &\left(\phi,\frac{\partial \mathbf{U}}{\partial \tau}+\mathbf{I}^M\frac{\partial \mathbf{U}}{\partial t}+\frac{\partial \mathbf{F}^j}{\partial x_j}+\frac{\partial \mathbf{G}^j}{\partial x_j}\right)=0 \\ &\Leftrightarrow\left(\phi,\frac{\partial \mathbf{U}}{\partial \tau}+\mathbf{I}^M\frac{\partial \mathbf{U}}{\partial t}\right)_\Omega+\left(\phi,\frac{\partial}{\partial x}\mathbf{F}^j\right)_\Omega+\left(\phi,\frac{\partial}{\partial x}\mathbf{G}^j\right)_\Omega \\ &+\left(\phi,n_j\left(\hat{\mathbf{F}}^{j}-\mathbf{F}^{j-}\right)+n_j\left(\hat{\mathbf{G}}^{j}-\mathbf{G}^{j-}\right)\right)_{\partial\Omega}+=0 \end{aligned} \tag{5}$$

Where

$\hat{\mathbf{F}}^j{}_{\partial\Omega}=\hat{\mathbf{F}}^j\left(\hat{\mathbf{F}}^{j-},\hat{\mathbf{F}}^{j+}\right)_{\partial\Omega}$ and $\hat{\mathbf{G}}^j{}_{\partial\Omega}=\hat{\mathbf{G}}^j\left(\hat{\mathbf{G}}^{j-},\hat{\mathbf{G}}^{j+}\right)_{\partial\Omega}$

are the numerical fluxes.

Here $(.,.)$ represents the normal L_2 inner product and third term is flux vector. In this problem the numerical flux for convective terms is calculated

by using the Lax-Friedrich flux and local discontinuous galerkin for viscous terms.

Here, we took the Kornwinder Dubiner function on straight sided triangle as the basis written in equation (5) (see figure 1 and 2):

$$\phi_{ij}(r,s)=\sqrt{\frac{2i+1}{2}}\sqrt{\frac{2i+2j+2}{2}}P_i^{0,0}\left(\frac{2(1+r)}{(1-s)}-1\right)P_j^{2i+1,0}(s) \tag{6}$$

where, $P^{\alpha,\beta}$ is orthogonal Jacobi polynomial. All straight sided triangles are the image of this triangle under the map:

$$\begin{pmatrix}x\\y\end{pmatrix}=-\left(\frac{r+s}{2}\right)\begin{pmatrix}v_x^1\\v_y^1\end{pmatrix}+\left(\frac{1+r}{2}\right)\begin{pmatrix}v_x^2\\v_y^2\end{pmatrix}+\left(\frac{1+s}{2}\right)\begin{pmatrix}v_x^3\\v_y^3\end{pmatrix} \tag{7}$$

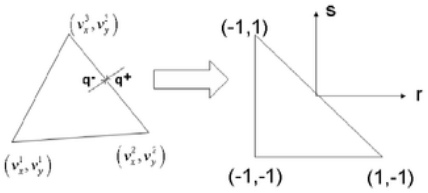

Figure 1: Coordinate transformation

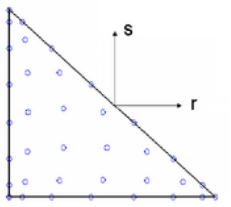

Figure 2: Seventh order Gauss Lobatto quadrature nodes

The vector $\mathbf{U}=(p \quad u \quad v)^T$ is expanded using equation (6), pressure is taken as example as follows:

$$p(r,s)=\sum_{i=0}^{N}\sum_{j=0}^{N-i}\phi_{ij}(r,s)\hat{p}_{ij} \tag{8}$$

$$p(r_n,s_n)=\sum_{m=1}^{m=M}\mathbf{V}_{nm}\hat{p}_m \tag{9}$$

$$\hat{p}_m=\sum_{m=1}^{m=M}\left(\mathbf{V}^{-1}\right)_{mj}p(r_j,s_j)$$

$$\begin{aligned}\frac{\partial p}{\partial r}(r,s)&=\sum_{i=0}^{N}\sum_{j=0}^{N-i}\frac{\partial\phi_{ij}}{\partial r}(r,s)\hat{p}_{ij}=\hat{\mathbf{D}}^r\mathbf{V}^{-1}p(r,s)\\ \frac{\partial p}{\partial s}(r,s)&=\sum_{i=0}^{N}\sum_{j=0}^{N-i}\frac{\partial\phi_{ij}}{\partial s}(r,s)\hat{p}_{ij}=\hat{\mathbf{D}}^s\mathbf{V}^{-1}p(r,s)\end{aligned} \tag{10}$$

$$\hat{\mathbf{D}}^r=\frac{\partial\phi}{\partial r}\ ;\ \hat{\mathbf{D}}^s=\frac{\partial\phi}{\partial s}$$

where $\mathbf{V}_{ij}$ and N are Vandermonde matrix and the order of Jacobi polynomial respectively.

The semi discrete of equation (5) can be written in the following form:

$$\frac{\mathrm{d}\mathbf{U}}{\mathrm{d}\tau}+\mathbf{I}^M\frac{\mathrm{d}\mathbf{U}}{\mathrm{d}t}=\mathbf{R} \tag{11}$$

A dual time stepping approach is employed for marching equation (12) in time. The real time t is discretized using second order implicit backward difference formula. The resulting equation becomes:

$$\frac{\mathrm{d}\mathbf{U}^{n+1}}{\mathrm{d}\tau}+\mathbf{I}^M\frac{\left(3\mathbf{U}^{n+1}-4\mathbf{U}^n+\mathbf{U}^{n-1}\right)}{2\Delta t}=\mathbf{R}^{n+1} \tag{12}$$

where superscript n denotes the current time level t, and n-1 refers to the previous time step t-Δt, while the unknowns are calculated at time t+Δt by n+1. Equation (12) can be written in a simpler form as:

$$\frac{\mathrm{d}\mathbf{U}^{n+1}}{\mathrm{d}\tau}=\overline{\mathbf{R}}^{n+1} \tag{13}$$

where $\overline{\mathbf{R}}$ contains the right hand side of equation (12) and the second term on left hand side of this equation. Equation (13) represents a pseudo-time evolution of flow field and has no physical meaning until the steady state in pseudo-time is reached.

The Equation (8) is integrated in pseudo-time marching by using five stage of fourth order 2N-storage Runge-Kutta scheme as developed by [8]. The final equations are found as written in Eqs. (14) and (15) :

$$\frac{\mathrm{d}\mathbf{U}}{\mathrm{d}\tau}=\overline{\mathbf{R}}(\tau,\mathbf{U}(\tau)) \tag{14}$$

$$\begin{aligned}d\mathbf{U}_j&=A_j d\mathbf{U}_{j-1}+d\tau\overline{\mathbf{R}}(\mathbf{U}_j)\\ \mathbf{U}_j&=\mathbf{U}_{j-1}+B_j d\mathbf{U}_j\end{aligned}\quad ;\quad j=1,5 \tag{15}$$

where $d\tau$ is the pseudo-time step. The vectors **A** and **B** are the coefficients that will be used to determine the properties of the scheme.

4. INITIAL AND BOUNDARY CONDITIONS

Initial and boundary conditions The governing equations (1) or (3) require initial condition to start the calculation as well as boundary conditions at every time step. In the calculations presented in this paper, the uniform free-stream values are use as initial conditions: $p = p_\infty$; $u_1 = u_{1\infty}$; $u_2 = u_{2\infty}$. For external flow applications, the far-field bound is placed far away from the solid surface. Therefore, the free-stream values are imposed at the far-field boundary except along the outflow boundary where extrapolation for velocity components in combination with $p = p_\infty$ is used. On the solid surface, the no-slip condition is imposed for velocity components: $u_1 = 0$; $u_2 = 0$. The surface pressure distribution is determined by setting the normal gradient of pressure to be zero:

$$\frac{\partial p}{\partial n} = 0$$

5. RESULTS AND DISCUSSION

The accuracy of the proposed method is demonstrated by solving incompressible flow past 2-dimensional circular cylinder. The Reynolds number is varied from 20 to 40 for steady flow and from 100 to 200 for unsteady flow. The computational domain for steady flow is rectangle (-15, 25) × (-15, 15) and for unsteady flow is (-20, 20) × (-20, 80) wherein a circular cylinder of diameter d =1 placed at (0, 0). The mesh consists of 1228 triangles for steady flow and 5092 triangles for unsteady flow. For all the calculation, we took a fixed order of polynomial N =4, Prandtl number is 0.717 and fixed artificial compressibility parameter is equal to unity.

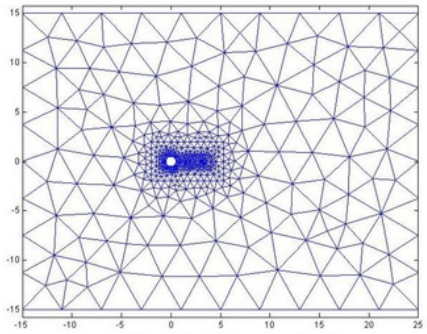

Figure 3a: Mesh for steady flow

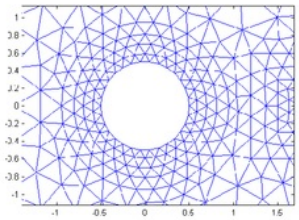

Figure 3b: Close-up mesh around cylinder for steady flow

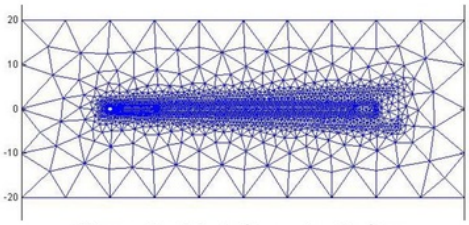

Figure 4a: Mesh for unsteady flow

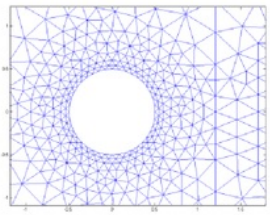

Figure 4b: Close-up mesh around cylinder for unsteady flow

Pseudo time step is $\Delta\tau$ = 0.0012 for steady flow. The results can be seen in figure 5 and 6. In front of object, pressure strongly varies and a region of high pressure is formed near separation point and two regions of low pressure are developed next. From figure 5, it can be seen the development of a recirculation zone behind the object with reverse velocity. Figure 5 and 6 give the computed

pressure for different values of Reynolds number (Re=20 and 40). As shown, the DG scheme gives excellent pressure stabilization, with the computed pressure contours being highly smooth and non-oscillatory.

The calculated results for steady flows are compared with the other numerical data. Table 1 compares the Drag coefficient (Cd). The agreement is quite good.

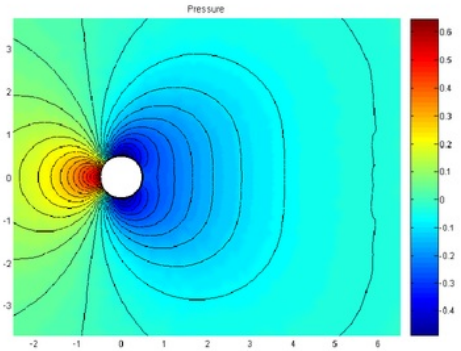

Figure 5a: Isobar of Re=20

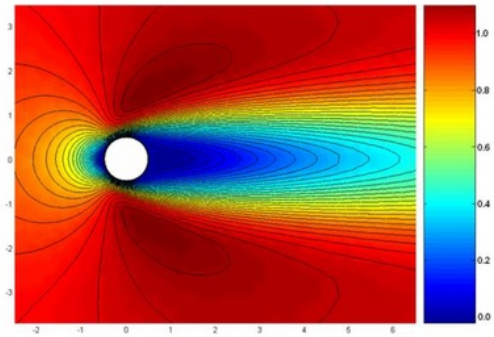

Figure 5b: Horizontal velocity of Re=20

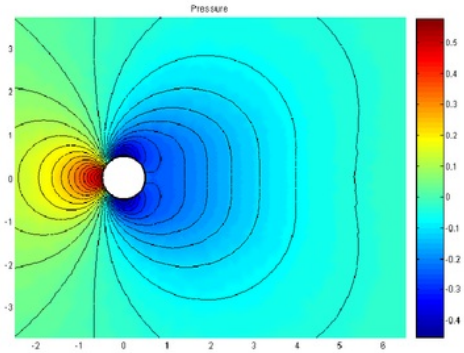

Fig. 6a. Isobar of Re=20

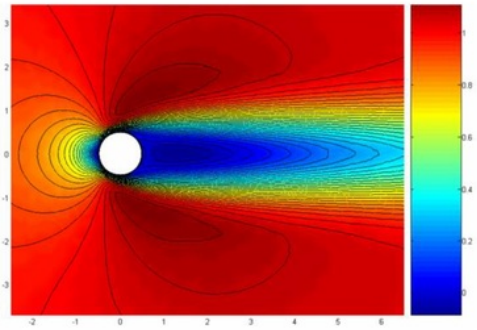

Figure 6b: Horizontal velocity of Re=20

Table 1. Drag coefficient (Cd) comparisons for steady flows

Author	Re=20	Re=40
Takami *et al.**	2.003	1.536
Dennis *et al.**	2.045	1.522
Tuann *et al.**	2.253	1.675
Ding *et al.**	2.180	1.713
Nithiarasu *et al.**	2.060	1.564
Thomas*	2.076	1.603
Present work	**2.040**	**1.527**

*: adapted from [9]

The ability of the discontinuous galerkin scheme with dual time-stepping to simulate transient flow is illustrated here by computing the vortex shedding in the wake of flow past a circular cylinder at Re = 100 and 200. This has been a popular test case for validating the transient part of numerical schemes. The problem is solved using is $\Delta t = 0.1$ and $\Delta\tau = 0.001$ and total of 250 pseudo-time iterations. Figure 7 provides a full simulation analysis of the Cl and Cd histories for each real time step on the mesh. As can be seen, once the initial transient stage has passed, the simulation settles down to an almost periodic convergence pattern. After the initial transient, each variable develops a periodic variation. This is due to the periodic shedding of vortices from behind the cylinder. This can be seen more clearly in figure 7, 8 and 9. A quantitative analysis of the results was also conducted and is shown Table 2. Generally, all the results shown for DG scheme are in good agreement with the other results.

Table 2: Cl, Cd and St comparisons for unsteady flows

Author	Re=100		
	Cl	Cd	St
Roger & Kwak [6]	±0.358	1.376 ±0.011	0.163
Pontaza [10]	±0.356	1.356	0.167
Mittal [11]	±0.356	1.386	0.169
Roshko (exp) [12]	-	-	-
Bintoro & Pranowo [13]	-	-	-
Rosenfeld [12]	-	-	-
Li [14]	-	-	-
Present work	**±0.3644**	**1.3440 ±0.013**	**0.1563**

Re=200		
Cl	Cd	St
	-	
±0.65	1.23±0.05	0.185
-	-	-
-	-	-
-	-	0.18
±0.552	1.24±0.09	0.17
±0.674	1.329±0.044	0.197
±1	1.17±0.15	0.18
±0.645	**1.311± 0.036**	**0.176**

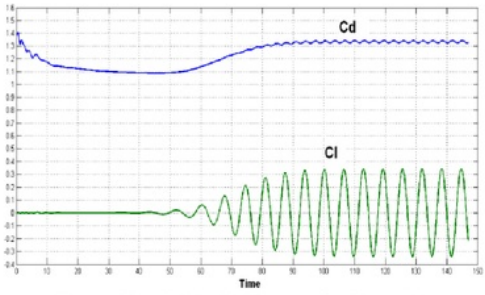

Figure 7a: Cd & Cl History for Re=100

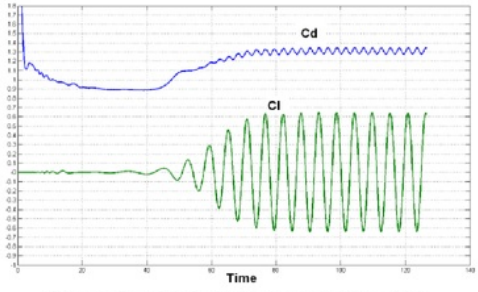

Figure 7b: Cd & Cl History for Re=200

The qualitative results are shown in figures 8 and 9. Here, the contours of pressure and vorticity are shown, for the real non-dimensional times of 100 and 120 respectively. All results are of high quality with no non-physical oscillations. The narrowing of the wake and the increase in shedding frequency, as the Reynolds number increases, is clear from these plots. We observe that at higher Reynolds numbers the vortices in the far-downstream wake coalesce and the region of coalescence moves upstream as the Reynolds number increases.

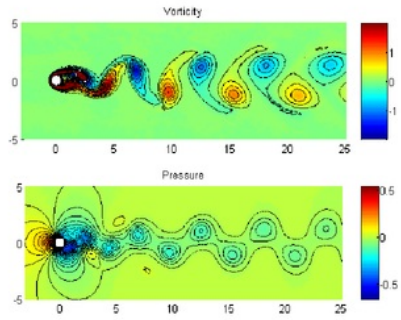

Figure 8a: Iso-vorticity and Isobar for Re=100 at t=100

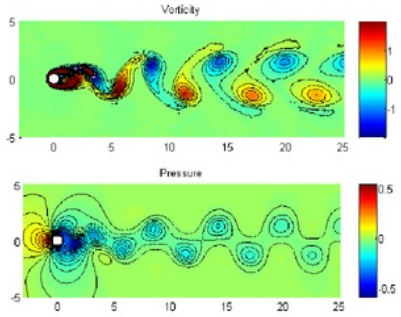

Figure 8b: Iso-vorticity and Isobar for Re=100 at t=120

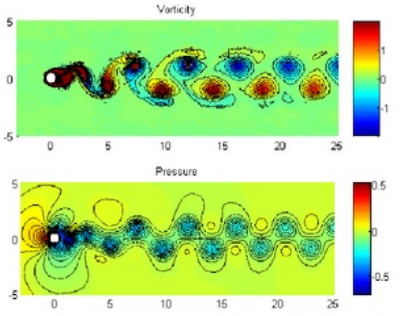

Figure 9a: Iso-vorticity and Isobar for Re=200 at t=100

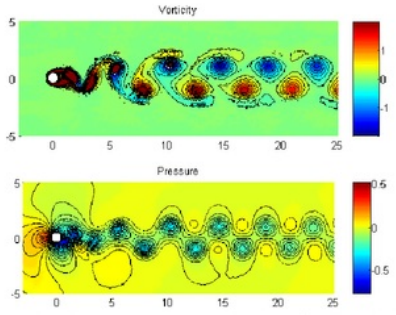

Figure 9a: Iso-vorticity and Isobar for Re=200 at t=120

It can be seen from the plots that the proposed method is stable for long time simulations. In addition, the plots show evidence that the outflow boundary condition allows for a smooth exit of the flow field and does not distort the flow upstream.

7. CONCLUSION

In this paper, we have presented a discontinuous galerkin method for steady and unsteady in artificial compressibility formulation connection with a dual time stepping approach. The method exhibits good numerical stability. The numerical results have a good agreement with the proposed experimental and numerical results reported in the previous studies.

ACKNOWLEDGMENT

We are very grateful to Prof. Hesthaven from Brown University USA for the valuable discussion and sharing his "Nudg" code.

REFERENCES

[1] M. T. Manzari, "A time-accurate finite element algorithm for incompressible flow problems", *International Journal of Numerical Methods for Heat & Fluid Flow,* Bradford: 2002. Vol.13 No.2, pp. 158-177.

[2] Pranowo and Deendarlianto, "Numerical solution of steady state free convection using unstructured discontinuous galerkin method". *Proceeding of the 3rd international conference on product design & development*, 12-13 December 2007, Jogjakarta, Indonesia

[3] A. J. Chorin, "Numerical method for solving incompressible viscous flow problem", *Journal of Computational Physics,* Vol. 2, pp. 12-26, 1967.

[4] M. T. Manzari, "An explicit finite element algorithm for convection heat transfer problems", *International Journal of Numerical Methods for Heat & Fluid Flow*, Bradford: 1999, Vol. 9-8, p. 860.

[5] F. Papa, et al., "A Numerical calculation of developing laminar flow in rotating ducts with a 180° bend", *International Journal of Numerical Methods for Heat & Fluid Flow*, Bradford: 2002, Vol.12 No.7, pp. 780-799.

[6] S. E. Rogers, and D. Kwak, "Steady and Unsteady Solutions of the incompressible Navier Stokes Equations", *AIAA Journal Part A*, Vol.29, No.4, pp. 603-610, 1991.

[7] N. T. Duc, "An implicit scheme for incompressible flow calculation with artificial compressibility method", *VNU Journal of Science, Mathematics-Physics.*, T. XXI, no. 4, 2005.

[8] M. H. Carpenter and C. A. Kennedy, "Fourth-order 2N-Storage Runge-Kutta Schemes", *NASA Technical Memorandum* 109112, 1994, NASA Langley Research Center, Hampton, Virginia.

[9] C. G. Thomas, "A locally conservative Galerkin (LCG) finite element method for convection-diffusion and Navier-Stokes equations", *Ph.D. Thesis*, 2006, University of Wales Swansea.

[10] J. P. Pontaza. "A least-squares finite element formulation for unsteady incompressible flows with improved velocity-pressure coupling", *Journal of Computational Physics* 217, pp. 563-588, 2006.

[11] S. Mittal, V. Kumar, and A. Raghuvanshi, "Unsteady incompressible flows past two cylinders in tandem and staggered arrangements", *International Journal for Numerical Methods in Fluids,* 1997, 25: 1315-1344

[12] M. Rosenfeld, "Grid refinement test of time periodic flows over bluff bodies", *Int. Journal of Fluid and Computers*, Vol. 23, no. 5, 1994.

[13] A. G. Bintoro, and Pranowo, "Perhitungan numeris pembebanan hidrodinamis aliran fluida laminar viskos tak tunak melewati silinder pada bilangan Reynold rendah", *Jurnal Teknologi Industri*, Vol. VI, April 2002.

[14] J. Li et al., "Numerical study of laminar flow past one and two circular cylinders", I*nt. Journal of Fluid and Computers*, Vol. 21, no. 3, 1991.

CCP_24

ORIGINALITY REPORT

26%	10%	26%	6%
SIMILARITY INDEX	INTERNET SOURCES	PUBLICATIONS	STUDENT PAPERS

PRIMARY SOURCES

1	International Journal of Numerical Methods for Heat & Fluid Flow, Volume 13, Issue 2 (2006-09-19) Publication	9%
2	www.emeraldinsight.com Internet Source	5%
3	Pontaza, J.P.. "A least-squares finite element formulation for unsteady incompressible flows with improved velocity-pressure coupling", Journal of Computational Physics, 20060920 Publication	3%
4	Park, Warn-Gyu, Young-Rae Jung, and Seong-Do Ha. "Numerical analysis of turbulent flows around a high-speed train including cross-wind effects", 14th Applied Aerodynamics Conference, 1996. Publication	3%
5	ntrs.nasa.gov Internet Source	3%

"Computational Fluid Dynamics 2006", Springer

6	Nature, 2009 Publication	2%
7	Proceedings of the Institute of Industrial Engineers Asian Conference 2013, 2013. Publication	2%

Exclude quotes	On	Exclude matches	< 2%
Exclude bibliography	On		

CCP_24

GRADEMARK REPORT

FINAL GRADE

/0

GENERAL COMMENTS

Instructor

PAGE 1

PAGE 2

PAGE 3

PAGE 4

PAGE 5

PAGE 6

PAGE 7

PAGE 8